

bands combination, such as using the NIR channel in place of the SWIR one, could help to face this issue within the zones characterized by sporadic snow events.

In any case, other test cases should be investigated in the next future to better assess the above-mentioned issues as well as to further confirm the quality of the results achieved in this work, considering other environmental scenarios as well as flooding events of a different nature and dynamics. Moreover, it should be stressed that a possible implementation of RST-FLOOD at global scale would require a consistent preliminary work, aimed first at collecting multiple-year time series homogeneous satellite records and then to their analyses in order to produce the reference fields.

Finally, it is worth noting that the proposed approach can also be exported on other VIIRS bands able to detect flooded area due to the differential nature of RST scheme. Thermal Moderate bands (i.e., M15: 10.263–11.263 μm ; M16: 11.538–12.488 μm) can be indeed used to identify inundated area by exploiting the difference in terms of thermal inertia (TI) that these areas should present respect with the unperturbed condition of the surrounding areas [63]. Water shows a higher TI than dry soil and consequently a less capability to change its temperature during the diurnal cycle. Therefore, those areas where soil water content increases because of the flood typically show a reduced diurnal temperature fluctuation compared to the dry conditions, with, in particular, a brightness temperature increase in night-time [64]. This physical property will allow also for a night-time flood detection that will enforce the potential of this sensor in providing near-real time and continuous information about flood dynamics.

In this framework, we have implemented the same approach described in Section 3.3 to analyse the VIIRS M15 image acquired on 4 December 2013 at 00:45, producing the corresponding RST-FLOOD map (Figure 14), where the anomalous pixels in terms of increasing $\text{ALICE}_{\text{TIR}}$ values are reported. Although the lower spatial resolution of these data (750 m) than the Imagery ones, the result is quite impressive, because all the anomalous pixels are located along the rivers in good agreement with the flood hazard map (Figure 4) and they are almost well co-located to the areas already detected (see Figure 10). It is worth noting that $\text{ALICE}_{\text{TIR}}$ value higher than 4 were not found and that, in the night-time images of the following days, flooded pixels were detected at ALICE values less than 2, hence resulting no statistically significant. The low spatial resolution of the thermal data, as well as a lower signal intensity in correspondence of flooded areas than the one measured at VNIR wavelengths, is probably at the basis of such a behaviour.

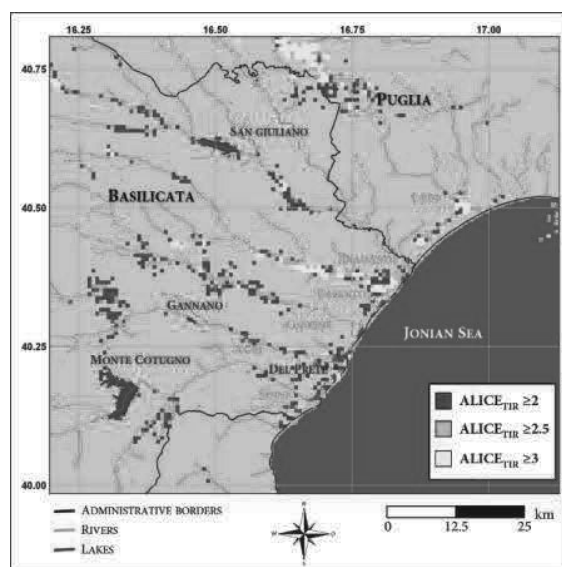


Figure 14. $\text{ALICE}_{\text{TIR}}$ map for the VIIRS data of 04/12/2013 at 00:45 GMT.

Considering that such a VIIRS image has been acquired almost 12 hours before the first diurnal one considered in the previous analysis, the integration of the maps referred to night-time (Figure 14) and daytime (Figure 10) conditions, further extends the investigated temporal domain.

6. Conclusions

The RST-FLOOD, a well-established satellite-based approach for flood detection and monitoring, has been fully implemented here for the first time with SNPP-VIIRS data. The event that affected the Metaponto Plain (southern Italy) during the first week of December 2013 has been investigated using such an approach by analysing 171 SNPP orbits, for a total of 684 VIIRS SDR products.

A study aimed at identifying the best signal, among the opportunities assured by the first three VIIRS Imagery bands, has been preliminarily performed identifying the NDSI ($I1 - I3 / I1 + I3$) as the metric with the best trade-off between reliability and sensitivity respect to the investigated event features. Such a signal has been then implemented within the RST-FLOOD approach, through the computation of the ALICE index aimed to investigate the flood dynamics in the 4–8 December 2013 period. The achieved findings demonstrated the good potential of the proposed approach in providing daily reliable indication on the flooding event. Only a residual 11.5% of possible false positives was recorded when the whole investigated scene was considered, reducing to only 4% when the area mostly affected by the event was investigated. An anomalous area of about 18 km², flooded “for sure” accordingly to the outcomes provided by previous works [31,37] as well as of the flood documentations [32–36], was detected by RST-FLOOD outside the flood hazard map, suggesting the need of its updating for better managing future risk, especially considering that an increase in intensity and in frequency of extreme meteo-hydrological events has expect in the next year for the Basilicata region [65]. The comparison with another VIIRS-based method [11], developed to work a global scale, confirmed the reliability of the outputs, suggesting a good capability of RST-FLOOD in detecting flooded area.

Finally, the achieved results demonstrated the potential of medium-resolution optical sensors, like VIIRS, in detecting floods that affect small watersheds, usually investigable only by using data (optical- or microwave-based) at higher spatial resolution [17]. Considering the high temporal resolution offered by VIIRS sensor (that thanks to the recent launch of JPSS-1 has further improved), the relevance of the achieved results become quite evident. The possibility of having continuous and reliable indication about the flood localization and extent may represent a valuable resource for both decision makers and hydrological models. Their assimilation would allow both for an updating of the model set up conditions as well as for a general quality improvement of the results. Finally, their integration with high spatial resolution optical data, such as those acquired by the MultiSpectral Instrument (MSI) aboard European Space Agency (ESA) Sentinel-2 mission, will allow for a more detailed view of the areas affected by the event.

Author Contributions: Conceptualization, T.L. and M.F.; Data curation, T.L., E.C., M.F. and V.S.; Formal analysis, T.L., E.C., M.F. and V.S.; Investigation, T.L. and M.F.; Methodology, T.L., M.F., N.P. and V.T.; Validation, M.F.; Visualization, T.L.; Writing—original draft, T.L. and M.F.; Writing—review & editing, N.P. and V.T..

Funding: This work has been partly funded in the framework of the MIUR SMART BASILICATA project.

Acknowledgments: We would like to acknowledge the Civil Protection of the Basilicata Region for providing river water level data.

Conflicts of Interest: The authors declare no conflict of interest.

References

1. Samela, C.; Albano, R.; Sole, A.; Manfreda, S. A GIS tool for cost-effective delineation of flood-prone areas. *Comput. Environ. Urban Syst.* **2018**, *70*, 43–52. [CrossRef]
2. Ward, P.J.; de Perez, E.C.; Dottori, F.; Jongman, B.; Luo, T.; Safaie, S.; Uhlemann-Elmer, S. The Need for Mapping, Modeling, and Predicting Flood Hazard and Risk at the Global Scale. In *Global Flood Hazard: Applications in Modeling, Mapping, and Forecasting*, 1st ed.; Schumann, G.J.-P., Bates, P.D., Apel, H., Aronica, G.T., Eds.; John Wiley & Sons, Inc.: Hoboken, NJ, USA, 2018; ISBN 978-1-119-21786-2.

3. Munich, R.E. Topics Geo—Natural Catastrophes 2017. Analyses, Assessments, Positions. 2018. Available online: https://www.munichre.com/site/touch-publications/get/documents_E711248208/mr/assetpool.shared/Documents/5_Touch/_Publications/TOPICS_GEO_2017-en.pdf (accessed on 12 February 2019).
4. Antonioli, F.; Anzidei, M.; Amorosi, A.; Presti, V.L.; Mastronuzzi, G.; Deiana, G.; Marsico, A. Sea-level rise and potential drowning of the Italian coastal plains: Flooding risk scenarios for 2100. *Quat. Sci. Rev.* **2017**, *158*, 29–43. [CrossRef]
5. Ward, P.J.; Jongman, B.; Aerts, J.C.J.H.; Bates, P.D.; Botzen, W.J.W.; Diaz, L.A.; Hallegatte, S.; Kind, J.M.; Kwadijk, J.; Scussolini, P.; et al. A global framework for future costs and benefits of river-flood protection in urban areas. *Nat. Clim. Chang.* **2017**, *7*, 642–646. [CrossRef]
6. Sun, D.; Li, S.; Zheng, W.; Croitoru, A.; Stefanidis, A.; Goldberg, M. Mapping floods due to Hurricane Sandy using NPP VIIRS and ATMS data and geotagged Flickr imagery. *Int. J. Digit. Earth* **2016**, *9*, 427–441. [CrossRef]
7. Huang, C.; Chen, Y.; Zhang, S.; Wu, J. Detecting, extracting, and monitoring surface water from space using optical sensors: A review. *Rev. Geophys.* **2018**, *56*, 333–360. [CrossRef]
8. Schumann, G.P.; Brakenridge, G.R.; Kettner, A.J.; Kashif, R.; Niebuhr, E. Assisting Flood Disaster Response with Earth Observation Data and Products: A Critical Assessment. *Remote Sens.* **2018**, *10*, 1230. [CrossRef]
9. Markert, K.L.; Chishtie, F.; Anderson, E.R.; Saah, D.; Griffin, R.E. On the merging of optical and SAR satellite imagery for surface water mapping applications. *Results Phys.* **2018**, *9*, 275–277. [CrossRef]
10. Dasgupta, A.; Grimaldi, S.; Ramsankaran, R.; Pauwels, V.R.N.; Walker, J.P.; Chini, M.; Hostache, R.; Matgen, P. Flood Mapping Using Synthetic Aperture Radar Sensors from Local to Global Scales. In *Global Flood Hazard: Applications in Modeling, Mapping, and Forecasting*, Geophysical Monograph 233, 1st ed.; John Wiley & Sons, Inc.: Hoboken, NJ, USA, 2018; ISBN 978-1-119-21786-2.
11. Li, S.; Sun, D.; Goldberg, M.D.; Sjöberg, B.; Santek, D.; Hoffman, J.P.; DeWeese, M.; Restrepo, P.; Lindsey, S.; Holloway, E. Automatic near real-time flood detection using Suomi-NPP/VIIRS data. *Remote Sens. Environ.* **2018**, *204*, 672–689. [CrossRef]
12. The International Charter Space and Major Disasters. Available online: <https://disasterscharter.org/web/guest/home> (accessed on 12 February 2019).
13. Copernicus Emergency Management Service. Available online: <https://emergency.copernicus.eu/> (accessed on 12 February 2019).
14. Lacava, T.; Ciancia, E.; Faruolo, M.; Pergola, N.; Satriano, V.; Tramutoli, V. Analyzing the December 2013 Metaponto Plain (Southern Italy) Flood Event by Integrating Optical Sensors Satellite Data. *Hydrology* **2018**, *5*, 43. [CrossRef]
15. Fayne, J.; Bolten, J.; Lakshmi, V.; Ahamed, A. Optical and Physical Methods for Mapping Flooding with Satellite Imagery. In *Remote Sensing of Hydrological Extremes*; Springer Remote Sensing/Photogrammetry; Lakshmi, V., Ed.; Springer International Publishing: Basel, Switzerland, 2017; Chapter 5; pp. 83–103. [CrossRef]
16. Kwak, Y. Nationwide Flood Monitoring for Disaster Risk Reduction Using Multiple Satellite Data. *ISPRS Int. J. Geo-Inf.* **2017**, *6*, 203. [CrossRef]
17. Ogilvie, A.; Belaud, G.; Massuel, S.; Mulligan, M.; Le Goulven, P.; Calvez, R. Surface water monitoring in small water bodies: Potential and limits of multi-sensor Landsat time series. *Hydrol. Earth Syst. Sci.* **2018**, *22*, 4349–4380. [CrossRef]
18. Lacava, T.; Ciancia, E.; Coviello, I.; Di Polito, C.; Faruolo, M.; Pergola, N.; Satriano, V.; Tramutoli, V. A Satellite Multi-Sensor Approach For Flooded Areas Detection and Monitoring. *Adv. Watershed Hydrol.* **2015**, *51*, 83–96.
19. Brakenridge, G.R. Flood Risk Mapping from Orbital Remote Sensing. In *Global Flood Hazard: Applications in Modeling, Mapping, and Forecasting*, 1st ed.; Schumann, G.J.-P., Bates, P.D., Apel, H., Aronica, G.T., Eds.; John Wiley & Sons, Inc.: Hoboken, NJ, USA, 2018; ISBN 978-1-119-21786-2.
20. Normandin, C.; Frappart, F.; Lubac, B.; Bélanger, S.; Marieu, V.; Blarel, F.; Robinet, A.; Guiastrennec-Faugas, L. Quantification of surface water volume changes in the Mackenzie Delta using satellite multi-mission data. *Hydrol. Earth Syst. Sci.* **2018**, *22*, 1543–1561. [CrossRef]
21. Tramutoli, V. Robust Satellite Techniques (RST) for Natural and Environmental Hazards Monitoring and Mitigation: Theory and Applications. In Proceedings of the Fourth International Workshop on the Analysis of Multitemporal Remote Sensing Images, Louven, Belgium, 18–20 July 2007. [CrossRef]

22. Lacava, T.; Filizzola, C.; Pergola, N.; Sannazzaro, F.; Tramutoli, V. Improving flood monitoring by the Robust AVHRR Technique (RAT) approach: The case of the April 2000 Hungary flood. *Int. J. Remote Sens.* **2010**, *31*, 2043–2062. [CrossRef]
23. Faruolo, M.; Coviello, I.; Lacava, T.; Pergola, N.; Tramutoli, V. A multi-sensor exportable approach for automatic flooded areas detection and monitoring by a composite satellite constellation. *IEEE Trans. Geosci. Remote Sens.* **2013**, *51*, 2136–2149. [CrossRef]
24. Imbrenda, V.; D’Emilio, M.; Lanfredi, M.; Macchiato, M.; Ragosta, M.; Simoniello, T. Indicators for the estimation of vulnerability to land degradation derived from soil compaction and vegetation cover. *Eur. J. Soil Sci.* **2014**, *65*, 907–923. [CrossRef]
25. Imbrenda, V.; Coluzzi, R.; Lanfredi, M.; Loperte, A.; Satriani, A.; Simoniello, T. Analysis of landscape evolution in a vulnerable coastal area under natural and human pressure. *Geomat. Nat. Hazards Risk* **2018**. [CrossRef]
26. Autorità di Bacino della Basilicata. Mappe della Pericolosità e Mappe del Rischio Idraulico, Relazione 2014. Available online: http://www.adb.basilicata.it/adb/Pstralcio/pianoacque/Relazione_ottobre_2014.pdf (accessed on 12 February 2019).
27. Autorità di Bacino della Basilicata. Capitolo IV, Disponibilità: Le Acque superficiali. 2016. Available online: <http://www.adb.basilicata.it/adb/pstralcio/bilancioidrico/cap4.pdf> (accessed on 12 February 2019).
28. Centro Funzionale Decentrato della Protezione Civile Basilicata. Dati in Tempo Reale—Pluviometria. 2018. Available online: <http://centrofunzionalebasilicata.it/it/sensoriTempoReale.php?st=I> (accessed on 12 February 2019).
29. Dal Sasso, S.F.; Cantisani, A.; Lanorte, V.; Pacifico, G.; Manfreda, S. Gli eventi storici della Basilicata. In *Le Precipitazioni Estreme in Basilicata*, 1st ed.; Manfreda, S., Sole, A., De Costanzo, G., Eds.; Universosud Società Cooperativa: Potenza, Italy, 2015; pp. 6–24. ISBN 978-88-99432-03-4. Available online: http://www.centrofunzionalebasilicata.it/it/pdf/pioggia_download.pdf (accessed on 12 February 2019).
30. Di Polito, C.; Ciancia, E.; Coviello, I.; Doxaran, D.; Lacava, T.; Pergola, N.; Satriano, V.; Tramutoli, V. On the Potential of Robust Satellite Techniques Approach for SPM Monitoring in Coastal Waters: Implementation and Application over the Basilicata Ionian Coastal Waters Using MODIS-Aqua. *Remote Sens.* **2016**, *8*, 922. [CrossRef]
31. D’Addabbo, A.; Refice, A.; Pasquariello, G.; Lovergine, F.P.; Capolongo, D.; Manfreda, S. A Bayesian network for flood detection combining SAR imagery and ancillary data. *IEEE Trans. Geosci. Remote Sens.* **2016**, *54*, 3612–3625. [CrossRef]
32. Centro Funzionale Decentrato della Protezione Civile Basilicata. Eventi Meteorologici Eccezionali dei Giorni 1, 2 e 3 Dicembre 2013 nel territorio della Regione Basilicata. 2013. Available online: http://www.centrofunzionalebasilicata.it/ew/ew_pdf/r/Report%20evento%20dicembre%202013.pdf (accessed on 12 February 2019).
33. Autorità di Bacino della Puglia. Valutazione Globale Provvisoria del Piano di Gestione del Rischio di Alluvioni. 2015. Available online: http://www.adb.puglia.it/public/files/downloads/20151104_PGRA/VGP.pdf (accessed on 12 February 2019).
34. Centro Funzionale Decentrato della Protezione Civile Puglia. Rapporto D’evento: Evento Meteo-Idropluviometrico del 30 Novembre–3 Dicembre 2013. 2014. Available online: <http://www.protezionecivile.puglia.it/archives/2244> (accessed on 12 February 2019).
35. Il Giornale della Protezione Civile Rassegna Stampa del 4/12/2013. 2013. Available online: <https://www.ilgiornaledellaprotezionecivile.it/html/download.html?id=7315738794M> (accessed on 12 February 2019).
36. Meteoweb. Maltempo, Esonda il Fiume Lato nel Tarantino: Case in Pericolo a Castellaneta Marina. 2013. Available online: <http://www.meteoweb.eu/2013/12/maltempo-esonda-il-fiume-lato-nel-tarantino-case-in-pericolo-a-castellaneta-marina/244468/#LL1PsEgcYY9bjUwO.99> (accessed on 12 February 2019).
37. De Musso, N.M.; Capolongo, D.; Refice, A.; Lovergine, F.P.; D’Addabbo, A.; Pennetta, L. Spatial evolution of the December 2013 Metaponto plain (Basilicata, Italy) flood event using multi-source and high-resolution remotely sensed data. *J. Maps* **2018**, *14*, 219–229. [CrossRef]
38. Joint Polar Satellite System (JPSS). JPSS-1 has a New Name: NOAA-20. 2017. Available online: <http://www.jpss.noaa.gov/launch.html> (accessed on 12 February 2019).

39. National Environmental Satellite, Data, and Information Service (NESDIS). Polar Satellite Programs Continuity of Weather Observations. 2018. Available online: https://www.nesdis.noaa.gov/sites/default/files/asset/document/Polar_Flyout%20Jan_2018_Weather_Signed_Linked.pdf (accessed on 12 February 2019).
40. Cao, C.; Xiong, J.; Blonski, S.; Liu, Q.; Upreti, S.; Shao, X.; Bai, Y.; Weng, F. Suomi NPP VIIRS sensor data record verification, validation, and long-term performance monitoring. *J. Geophys. Res. Atmos.* **2013**, *118*, 664–678. [CrossRef]
41. NOAA Comprehensive Large Array-data Stewardship System (CLASS). 2019. Available online: <https://www.avl.class.noaa.gov/saa/products/welcome> (accessed on 12 February 2019).
42. Polar2Grid, 2018. Available online: <https://www.ssec.wisc.edu/software/polar2grid/#> (accessed on 12 February 2019).
43. Geoportale Nazionale—Ministero dell’Ambiente e della Tutela del Territorio e del Mare. 2018. Available online: <http://www.pcn.minambiente.it/mattm/direttiva-alluvioni/> (accessed on 12 February 2019).
44. Community Satellite Processing Package (CSPP). Suomi-NPP VIIRS Flood Detection Software Version 1.0 Release. 2018. Available online: http://cimss.ssec.wisc.edu/cspp/viirs_flood_v1.0.shtml (accessed on 12 February 2019).
45. USGS Earth Explorer. Available online: <https://earthexplorer.usgs.gov/> (accessed on 12 February 2019).
46. Quinn, J.W. Landsat Band Combination. Available online: <http://web.pdx.edu/~emch/ip1/bandcombinations.html> (accessed on 12 February 2019).
47. USGS Landsat Missions. Available online: <https://landsat.usgs.gov/known-issues> (accessed on 12 February 2019).
48. Sole, A.; Giosa, L.; Copertino, V. Risk flood areas, a case study: Basilicata Region. *WIT Trans. Ecol. Environ.* **2017**, *104*, 213–228. Available online: <https://www.witpress.com/Secure/elibRARY/papers/RM07/RM07021FU1.pdf> (accessed on 12 February 2019). [CrossRef]
49. Tramutoli, V. Robust AVHRR Techniques (RAT) for Environmental Monitoring: Theory and applications. Earth Surface Remote Sensing II, Giovanna Cecchi, Eugenio Zilioli, Editors. *Proc. SPIE* **1998**, *3496*, 101–113.
50. Ciancia, E.; Coviello, I.; Di Polito, C.; Lacava, T.; Pergola, N.; Satriano, V.; Tramutoli, V. Investigating the chlorophyll-a variability in the Gulf of Taranto (North-western Ionian Sea) by a multi-temporal analysis of MODIS-Aqua Level 3/Level 2 data. *Cont. Shelf Res.* **2018**, *155*, 34–44. [CrossRef]
51. Koeppen, W.C.; Pilger, E.; Wright, R. Time series analysis of infrared satellite data for detecting thermal anomalies: A hybrid approach. *Bull. Volcanol.* **2011**, *73*, 577–593. [CrossRef]
52. Cuomo, V.; Filizzola, C.; Pergola, N.; Pietrapertosa, C.; Tramutoli, V. A self-sufficient approach for GERB cloudy radiance detection. *Atmos. Res.* **2004**, *72*, 39–56. [CrossRef]
53. Pietrapertosa, C.; Pergola, N.; Lanorte, V.; Tramutoli, V. Self Adaptive Algorithms for Change Detection: OCA (the One-channel Cloud-detection Approach) an adjustable method for cloudy and clear radiances detection. In Proceedings of the Technical Proceedings of the Eleventh International (A)TOVS Study Conference (ITSC-XI), Budapest, Hungary, 20–26 September 2000; pp. 281–291.
54. Huang, C.; Chen, Y.; Wu, J.; Li, L.; Liu, R. An evaluation of Suomi NPP-VIIRS data for surface water detection. *Remote Sens. Lett.* **2015**, *6*, 155–164. [CrossRef]
55. Xiao, X.G.; Shen, Z.X.; Qin, X.G. Assessing the potential of vegetation sensor data for mapping snow and ice cover: A Normalized Difference Snow and Ice Index. *Int. J. Remote Sens.* **2001**, *22*, 2479–2487. [CrossRef]
56. Boschetti, M.; Nutini, F.; Manfron, G.; Brivio, P.A.; Nelson, A. Comparative Analysis of Normalised Difference Spectral Indices Derived from MODIS for Detecting Surface Water in Flooded Rice Cropping Systems. *PLoS ONE* **2014**, *9*, e88741. [CrossRef]
57. Piper, M.; Bahr, T. A rapid cloud mask algorithm for SUOMI NPP VIIRS imagery EDRS. The International Archives of the Photogrammetry, Remote Sensing and Spatial Information Sciences. In Proceedings of the 36th International Symposium on Remote Sensing of Environment, Berlin, Germany, 11–15 May 2015; Volume XL-7/W3.
58. Candra, D.S.; Phinn, S.; Scarth, P. Cloud and cloud shadow masking using multi-temporal cloud masking algorithm in tropical environmental. The International Archives of the Photogrammetry, Remote Sensing and Spatial Information Sciences. In Proceedings of the XXIII ISPRS Congress, Prague, Czech Republic, 12–19 July 2016; Volume XLI-B2. [CrossRef]

59. Zhu, Z.; Woodcock, C.E. Object-based cloud and cloud shadow detection in Landsat imagery. *Remote Sens. Environ.* **2012**, *118*, 83–94. [CrossRef]
60. Sanyal, J.; Lu, X.X. Application of Remote Sensing in Flood Management with Special Reference to Monsoon Asia: A Review. *Nat. Hazards* **2014**, *33*, 283–301. [CrossRef]
61. Franci, F.; Mandanici, E.; Bitelli, G. Remote sensing analysis for flood risk management in urban sprawl contexts. *Geomat. Nat. Hazards Risk* **2015**, *6*, 583–599. [CrossRef]
62. Lacava, T.; Brocca, L.; Coviello, I.; Faruolo, M.; Pergola, N.; Tramutoli, V. Integration of optical and passive microwave satellite data for flooded area detection and monitoring. In *Engineering Geology for Society and Territory*; Springer International Publishing: Basel, Switzerland, 2014; Volume 3, pp. 631–635. [CrossRef]
63. Tramutoli, V.; Claps, P.; Marella, M.; Pergola, N.; Sileo, C. Feasibility of hydrological application of thermal inertia from remote sensing. In Proceedings of the 2nd Plinius Conference on Mediterranean Storms, Siena, Italy, 16–18 October 2000; pp. 16–18.
64. Verstraeten, W.W.; Veroustraete, F.; van der Sande, C.J.; Grootaers, I.; Feyen, J. Soil moisture retrieval using thermal inertia, determined with visible and thermal spaceborne data validated for European forests. *Remote Sens. Environ.* **2006**, *101*, 299–314. [CrossRef]
65. Piccarreta, M.; Pasini, A.; Capolongo, D.; Lazzari, M. Changes in daily precipitation extremes in the Mediterranean from 1951 to 2010: The Basilicata region, Southern Italy. *Int. J. Climatol.* **2013**, *33*, 3229–3248. [CrossRef]



© 2019 by the authors. Licensee MDPI, Basel, Switzerland. This article is an open access article distributed under the terms and conditions of the Creative Commons Attribution (CC BY) license (<http://creativecommons.org/licenses/by/4.0/>).